INVESTIGATING SNOWPACK VOLUMES AND ICING DYNAMICS IN THE MORAINE OF AN ARCTIC CATCHMENT USING UAV PHOTOGRAMMETRY

Éric Bernard* (eric.bernard@univ-fcomte.fr)

CNRS, University of Franche Comté, UMR ThéMA, Besançon, France

J. M. Friedt (jmfriedt@femto-st.fr)

CNRS, University of Franche Comté, UMR FEMTO-ST, Besançon, France

F. Tolle (florian.tolle@univ-fcomte.fr)
M. Griselin (madeleine.griselin@univ-fcomte.fr)

CNRS, University of Franche Comté, UMR ThéMA, Besançon, France

Ch. Marlin (christelle.marlin@u-psud.fr)

University of Paris-Sud 11, UMR GEOPS, Orsay, France

A. Prokop (alexander.prokop@unis.no)

Arctic Geology Department, The University Centre in Svalbard, UNIS, Norway

*Corresponding author

Abstract

Methods for assessing the contribution of the proglacial moraine into the water budget of an Arctic glacier are investigated. High spatial resolution elevation models at different seasons are needed to estimate the volume of ice and snow accumulated during winter in this part of the catchment basin and released into rivers during the melting season. Lidar currently provides the highest resolution for the generation of digital elevation models (DEMs). This paper considers the complementary use of a commercial off-the-shelf DJI Phantom 3 Professional unmanned aerial vehicle (UAV) for acquiring aerial photography, combined with structure-from-motion (SfM) analysis, for DEM computation. DEM differences between datasets acquired in April (maximum snow accumulation) and September (minimum snow cover) yield a volume difference attributed either to snow cover or icing formation. Repeated measurements over a short period highlight the processes of snow-cover storage in the moraine and melting dynamics.

KEYWORDS: Arctic, photogrammetry, proglacial moraine, SfM, snow cover, UAV

INTRODUCTION

THE ARCTIC IS ONE OF THE REGIONS most affected by current climate change (Hagen et al., 2003; Oerlemans, 2005). It is thus a reliable indicator for quantifying these changes through its hydro-glaciological dynamics (Hock, 2003; Hagen et al., 2005; Whitehead et al., 2014). In such dynamics, snow-related processes are considered to be a key parameter (Wright, 2005), especially considering its extreme variability due to air temperature shifts and increased precipitation (Eckerstorfer and Christiansen, 2011). Demonstrated effects of rain events on the snowpack (Nowak and Hodson, 2013; Schöber et al., 2014) show the importance of carefully examining the resulting dynamics. It directly impacts melting processes and proglacial hydrological dynamics as well (Bavay et al., 2013; Bernard et al., 2013). Hence, assessing the hydrological budget of a glacier basin requires measuring the contribution of its three geographical areas:

(1) *The glacier itself*. Snowpack quantification is quite easy due to the homogeneous topography of the glacier's surface. Snow height is measured on each accumulation/ablation stake providing specific mass balance (maximum snow accumulation on the glacier), and interpolated on its surface.
(2) *The surrounding slopes*. These are assumed to be a significant provider of snow due to the increase of avalanche activity. Nevertheless, monitoring slopes is quite difficult due to high instability, unless remote methods of measurements are used such as laser scanning.
(3) *The proglacial moraine*. This is positioned as a transfer interface, exhibiting dynamics which generate an increase in its change of geometry, both in quantity and frequency. The complex topography makes observation and measurement difficult, although necessary.

This paper focuses on this third area, which is the main interface between the glacier and its outlets. The work presented here deals with the quantification of proglacial moraine snowpack and icings. The observed climatic trend is indeed remarkable, not only through moraine morphological changes (Rachlewicz, 2010; Wiesmann et al., 2012), but also in the changing snowpack dynamics and properties. This is directly linked to the increase of both temperature and precipitation that have an immediate impact on the snowpack. Alongside this, the actual processes of glacial retreat consequently release a significant proglacial moraine expansion (Radić et al., 2014; Sobota, 2016). As a consequence, the moraine snowpack increases, modifying the water-stock balance. Considering these points, it is then necessary to estimate, in the same way as on the glacier and the slopes, the water equivalent represented by the snowpack in the moraine.

Therefore, observing and quantifying these processes is a key point but remains problematic: slopes and moraine are challenging environments where the unstable brittle materials present are unsuitable for distributing sensors, while the rough topography of the moraine prevents the use of interpolation (Bernard et al., 2017). Indeed, the snow and icing distribution in the moraine exhibits heterogeneities, such as snow-drift accumulation and channels filled with snow and/or ice; their scales of the same order of magnitude as the topographic variation, typically in the metre range. Furthermore, due to permanent morphological changes on the new deglaciated moraine, it is not possible to process data with the same references. This investigation focuses on the latter part of the budget: mapping snow and ice distribution in the moraine requires a high, sub-metre, spatial resolution in both lateral directions and decimetre resolution in the altitude measurement.

Hence, this research has considered flexible methods of data acquisition through structure-from-motion (SfM) digital image processing from photographs acquired from an unmanned aerial vehicle (UAV). This leads to the generation of high-resolution digital elevation models (DEMs) within short time frames, and differences of DEMs for estimating snow and icing distribution in the moraine. The underlying goal is to assess the use of combining SfM and UAVs as an efficient workflow to map and quantify cryosphere dynamics into a proglacial moraine, in a context of fast climate-induced morphologic changes.

In this paper, results are presented from snowpack and icing quantification over the Austre Lovénbreen, Svalbard, proglacial moraine. Repeated UAV surveys were conducted in the autumn of 2015 and spring of 2016, with simultaneous field-based observations and lidar acquisitions. This enables an innovative method to quantify solid water stock and snowpack dynamics in a deglaciating Arctic catchment.

GEOGRAPHICAL SETTING

The Arctic glacial basin considered in this investigation, Austre Lovénbreen, is located on the west coast of Svalbard on the Brøgger peninsula (79°N). This case study consists of a small land-terminating valley and polythermal glacier in a $10 \cdot 58$ km^2 basin (Fig. 1). Since the Little Ice Age (LIA), Austre Lovénbreen has been increasingly exposing forefield sediments to the processes of mobilisation and redistribution. Its proglacial moraine has thus grown continuously, today representing nearly 25% of the whole basin, with direct consequences on snowpack distribution and melting processes.
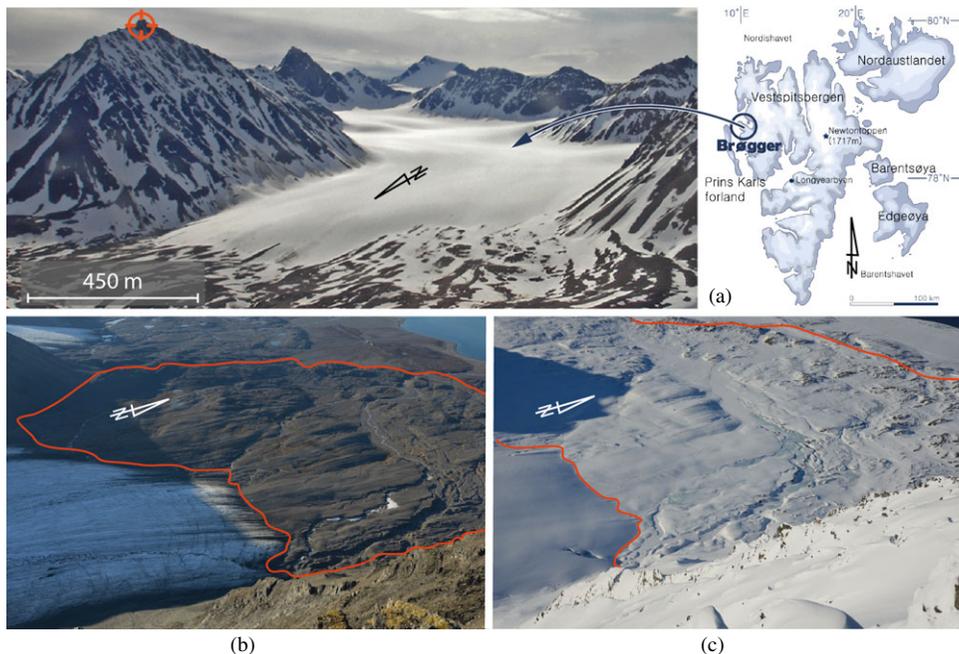

FIG. 1. (a) The fieldwork was located on the west coast of Spitsbergen. Proglacial moraine shown free of snow in summer (b) and in spring at its maximum snow accumulation (c). Photographs (b) and (c) were taken from the Haavimbfjellet summit pointing west, in August and April 2016.

This highly dynamic environment, constitutes a snowpack base which is much more complex than the glacier topography itself. Snow cover on the proglacial moraine is taking increasing importance compared to the snow cover on the glacier, changing the hydrological equation. As another consequence, quantification of this snow cover is quite problematic, and subject to significant spatio-temporal variability. To assess photogrammetric methods of quantification, several representative test areas on the moraine were chosen in order to compare different datasets.

Rᴇsᴇᴀʀᴄʜ Mᴇᴛʜᴏᴅs

Terrestrial Laser Scanning as a Reference

Terrestrial measurement methods, whether photogrammetric or lidar-based topography mapping, are all plagued by excessive cast-shadow effects from the grazing angle of measurements. Throughout this investigation, the reference will be lidar scans acquired from Haavimbfjellet (783 m above sea level), a summit overlooking the glacier front as well as the whole proglacial moraine under investigation. Acquisitions were performed in April and August 2016. For over a decade, terrestrial lidar has been extensively used for snow-depth mapping and allows for accuracies at the sub-decimetre scale (Prokop, 2008; Prokop et al., 2008, 2015; Deems et al., 2013). The position chosen allows for limited shadow effects in the region exhibiting the strongest morphological variation, namely the outlet of a sub-glacial stream. Lidar is, however, reluctantly considered for repeated mapping of the moraine area due to the challenge of bringing a cumbersome and fragile instrument into a physically demanding mountain environment. Nevertheless lidar, as an active method, operates independently of lighting conditions and only requires a clear atmosphere for light pulses to propagate unhindered. This is a significant advantage in the Arctic environment, characterised by a low-lying sun in the autumn period prior to the Arctic night and hence strong projected shadows challenging SfM processing (Fig. 2). All measurements were completed using a Riegl VZ-6000 laser scanner, operating at a wavelength of 1064 nm, selected for its strong reflectivity when illuminating snow- and ice-covered surfaces, with a measurement range sufficient to cover the maximum distance of 2500 m between the summit where the laser scanner is located during data acquisition and the furthest area of interest on the moraine (the main outlet of the basin). A point density of at least 15 samples/m^2 was collected in this dataset, with a significant variation due to the pronounced tangential angle of incidence. Non-ground points were filtered using the wedge filtering approach (Panholzer and Prokop, 2013). For referencing the two surfaces with respect to each other to calculate snow depths, an iterative closest point (ICP) algorithm was used (Prokop and Panholzer, 2009). The accuracy of the lidar measurements was determined by reproducibility tests of the snow-free areas and are in the order of 10 cm.

UAV Data Acquisition and Processing

A UAV represents the best compromise for quality data acquisition, specifically when high spatio-temporal repeatability is needed (Westoby et al., 2012; Lucieer et al., 2014b). The images were acquired from a commercial off-the-shelf (COTS) UAV system, selected for its ease of deployment – the aircraft and associated control systems fit in a lightweight backpack easily transported when walking on the moraine – while the low cost allows risking flight in challenging conditions. The DJI Phantom 3 Professional and Advanced have demonstrated appropriate characteristics to the mapping task (Bangen et al., 2014; Kršák et al., 2016; Cook,
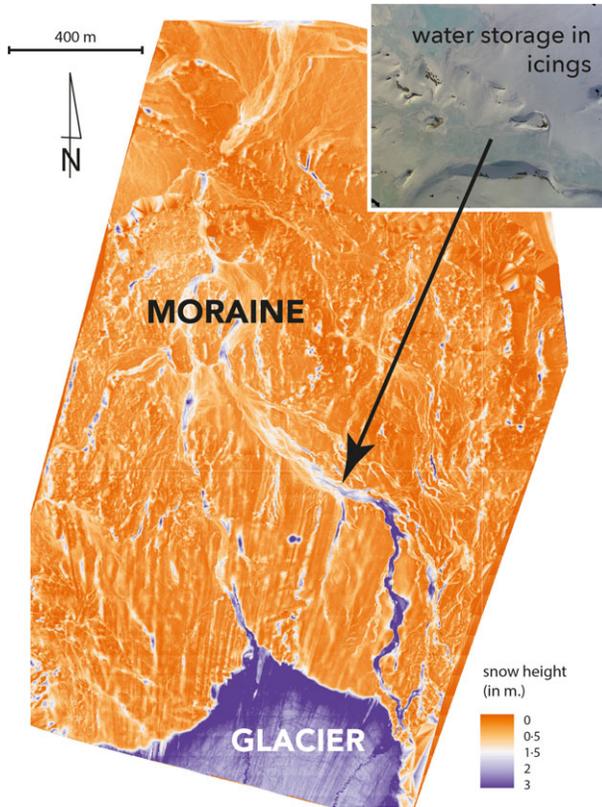
Fɪɢ. 2. Lidar map of elevation differences between summer (August) and winter (April) digital elevation models. Notice that the point cloud used to generate the DEM difference covered the whole moraine area in a single acquisition. The bottom dark-blue area is the glacier exhibiting strong ablation during the summer, while the light-blue coloured areas are the moraine with little elevation change, since spring 2016 exhibited low snow cover. Orange areas contain differences less than 1 m.

2017). This UAV has an integral Sony EXMOR f/2.8 digital camera with 4000×3000 pixels and a 94° field of view. The flying height was set to between 100 and 110 m, providing a ground sample distance (GSD) of 5 cm when considering the optical system's properties. The 15-minute autonomy at temperatures around 0°C and the horizontal speed of 10 m/s allowed for covering a flight-path length of about 9 km. The targeted 80% forward overlap between adjacent images, along the fast raster-scan axis, yields a coverage of about 700 to 1000 m by 400 m. Hence, most relevant parts of the 4 km^2 moraine were mapped with 10 flights (sorties) lasting 15 minutes each, totalling less than half a day of activity. The significance of this aspect lies in the ability to process the dataset for generating orthophotographs and DEMs under the assumption that no significant changes appear over such a short time period, other than shadow casts which prevent the matching of photographs of rough terrain imaged over time intervals of more than an hour.

UAV flight sessions were prepared by analysing the area of interest on a background satellite image in order to locate the flight limits. At the time of acquisition, no efficient software or application was available for UAV flight planning, making the acquisition process

less than optimal (Cook, 2017). Thus, manual flight control was selected to adapt the flight lines in real time to features seen on the ground by the operator (Fig. 3). Indeed, the limited battery life at low temperatures and short fine-weather window requires making choices about the observed area. Thus, the operator focused on active areas (exhibiting significant topographic features and dynamics), instead of performing a systematic overall raster-scan flight path. Furthermore, the Altizure software, used later to automate flight paths, was not readily functional and fully tested at these early flight dates, when optimal flight conditions (altitude, horizontal speed and the ability to track long and narrow features of interest – such as canyons in which ice and snow accumulate) were still being investigated.

Moreover, the set-up was used without prior camera calibration but the photographs were visually assessed on the basis of quality and overlap (in Agisoft PhotoScan), viewing angle and to remove blurred and under- or over-exposed images from further processing and analyses, as recommended by Lucieer et al. (2014a), Nolan et al. (2015) and Gindraux et al. (2017). Real-time video feedback allows for identifying features of interest on the ground, while the map displaying the global navigation satellite system (GNSS) position of the UAV during flight over the background image provides an indication of the area covered. The forward overlap of successive images, aimed at 80% to 60% for SfM processing, was selected by manually triggering the onboard camera: considering a horizontal speed of 10 m/s, a flying height of 100 m and a field of view of 66° along the short (3000 pixel) photograph axis (in the flight direction), each photograph spans a length of 130 m, so that an 80% overlap requires that the UAV has flown less than 26 m along its path, hence requiring an exposure once every 3 seconds at most. Thus, a 15-minute flight will generate about 300 photographs for processing.
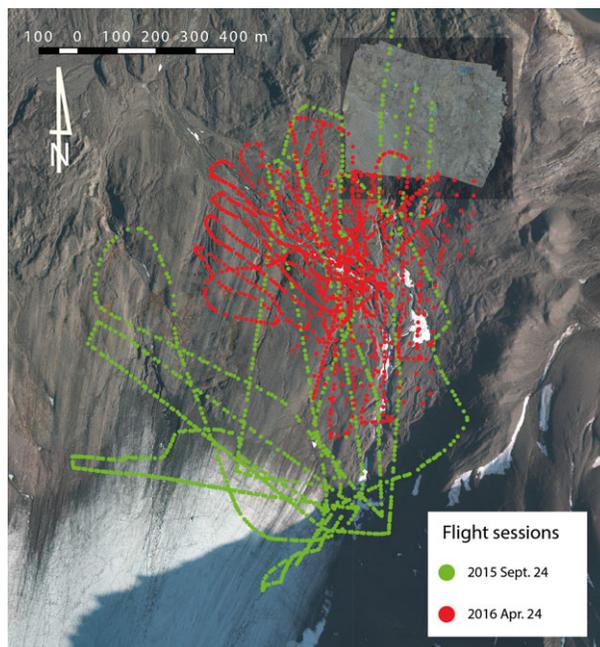

FIG. 3. Two manual flight paths for September 2015 and April 2016. The dots represent the GNSS position of each acquired photograph over features of interest.

The lateral overlap (sidelap) is aligned with the long (4000 pixel) picture axis. The distance from one track to an adjacent flight line is visually estimated on the map and is the strongest limitation of using the manual flight mode. While such an operating procedure allows adaption to ground features observed during flight – such as following a stream bed or valley of interest – it is less favourable to quantitative post-analysis over a wide area if the lateral overlap between adjacent tracks is not sufficient. Such a case is observed in Fig. 3, in which the path of the UAV flying over the glacier and returning back towards the moraine was not sharp enough for the two adjacent paths to overlap over the glacier. SfM processing achieved using MicMac (micmacIGN, 2017) was nevertheless able to handle the missing images and generated usable DEMs and orthophotographs, albeit with a hole of missing information where overlapping photographs were not available. As an example of a result of such an acquisition, Fig. 4 compares an aerial image provided by the Norwegian Polar Institute (2010) as a web map tile service (WMTS) with orthophotographs generated from the flight datasets from the Phantom 3 UAV.

DEM differencing requires sub-metre matching of successive acquisitions: the coarse acquisition L1 GNSS receiver used to control the UAV and tagging each acquired photograph only provides ± 5 m accuracy (Fig. 5). The point cloud, orthophotograph and DEM are positioned using a weighted balance between photogrammetric processing and GNSS camera positioning (from the UAV), with results depending on the practical implementation of the SfM algorithms and the weight given to the georeference tag associated with each photograph. These investigations have focused on the comparison of the commercial PhotoScan software from Agisoft and open-source MicMac available from the French Institut Géographique National (IGN). The same dataset was processed using a similar workflow in both software packages resulting, in both cases, in the same products: namely an orthophotograph and a DEM. This work was less interested in the point-cloud density, as this has been investigated already (Niederheiser et al., 2016), than with the positioning accuracy.

MicMac is quite involved during the tie-point search in image pairs, modelling the lens properties and locating the camera positions, as each picture was acquired based on photogrammetric processing. In the case of this small data subset of 40 images used for comparing both processing software, 15 pictures were selected to identify the parameters of

(a)   (b)
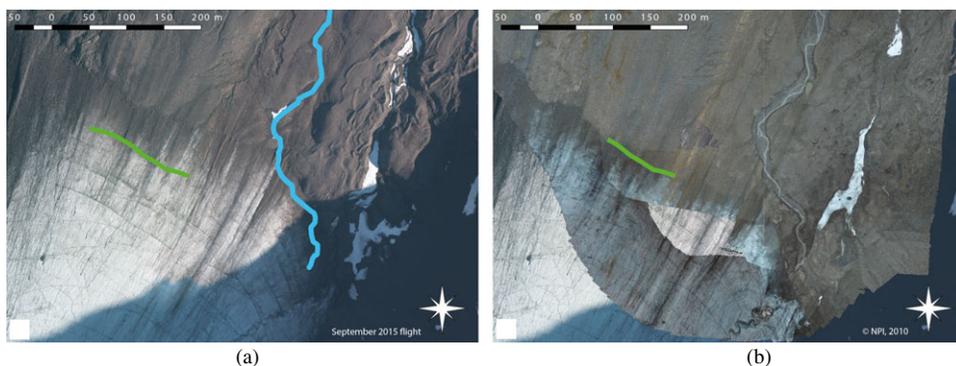
Fig. 4. Comparison of: (a) an orthophotograph available on the Norsk Polar Institute WMTS server acquired in 2010; and (b) an orthophotograph assembled from images acquired from a UAV in September 2015. The green lines are a guide to the 2015 glacier-front position, emphasising glacier retreat. A sub-glacial stream, shown as a blue line in (a), is carving a new canyon in the newly deglaciated moraine area, as visible in (b).
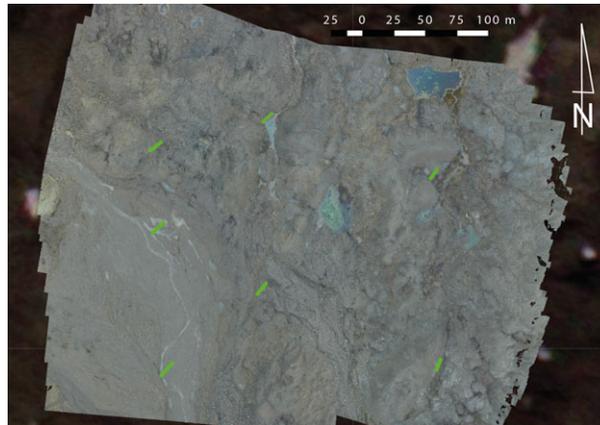
FIG. 5. Assessment of the discrepancies using two different software programs on the same dataset. The orthophotograph of the area under consideration has green lines indicating the shift between features found on the two orthophotographs generated using IGN MicMac and Agisoft PhotoScan. This is generated from the same dataset of photographs annotated with the same GNSS positions found in the Exif header. The typical shift (green lines) is 10 m.

the eight degrees of freedom in the standard radial lens model (Pierrot-Deseilligny, 2017), yielding a residual error of 0·82 pixel with a worst case of 0·89 pixel. Locating the cameras for the whole dataset when using this initial lens model yielded a residual error of 0·91 pixel with a worst case of 1·25 pixel.

While the general trend of the geometry between the orthophotographs generated by the two software packages is a fairly consistent north-east to south-west offset, some discrepancy remains even after adjusting this coarse offset. In order to readjust images and to improve the measurement accuracy, ground control points (GCPs) using natural features were used, such as easily identifiable erratic boulders. In the latter strategy, one DEM is selected as a reference and the second DEM is moved to match features visible on the associated orthophotograph. Considering that the lidar DEM is a reference, different SfM processing software yields different georeferencing accuracy when using the same camera providing GNSS coordinates for positioning the DEM. Indeed, after translating one orthophotograph along the vector defined by one of the green lines visible in Fig. 5, the remaining offsets are in the 2·5 m range at the opposite corner to the one in which the reference line was selected. The resulting DEMs are either adjusted using ground-based control points or matching features after acquisition by analysing the orthophotographs.

Assuming an airborne lidar dataset recorded in August 2003 (Rees and Arnold, 2007) provides the utmost positioning accuracy, this research assessed the photogrammetrically generated DEM positioning accuracy with respect to this reference dataset. According to Arnold et al. (2006), this lidar dataset was acquired at an altitude of 1600 m above sea level, giving a variable height above ground from 1600 m at the coast, to approximately 500–600 m above the peaks at the southern end of the catchment area. Fig. 6 provides a cross section comparing the elevation between the various DEMs. Computing standard deviations at distances of 82 and 310 m along the cross section on the elevation differences yields $\sigma_z = 0·6$ m between the airborne lidar and the PhotoScan-generated DEM, $\sigma_z = 0·7$ m between airborne lidar and the MicMac-generated DEM, and $\sigma_z = 0·9$ m between the two photogrammetrically generated DEMs. The doming of the surfaces generated by photogrammetric processing
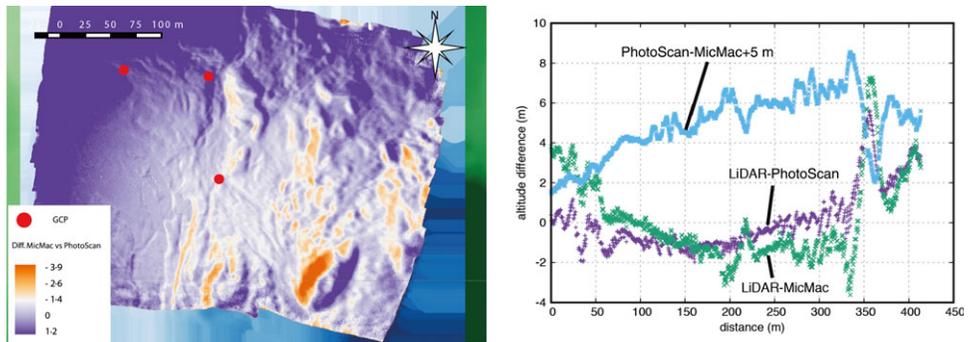
FIG. 6. Left: map of the DEM difference. The positioning mismatch is obvious in the lower-right corner where a hill exhibits a positive height difference on the right and negative height difference on the left. Right: cross section of DEM differences between the airborne lidar dataset and two DEMs generated from photogrammetric processing of the same pictures with the same camera GNSS coordinates provided in each picture Exif header, using Agisoft PhotoScan and MicMac. So that the graph is readable, +5 m was added to the PhotoScan–MicMac difference.

(Wackrow and Chandler, 2008; 2011; James and Robson, 2014; Eltner and Schneider, 2015) is visible on the UAV-generated DEM subtracted from the lidar DEM, the latter not being affected by such lens-modelling distortion effects. The effect is compensated for when subtracting two DEMs generated by independent photogrammetric processing software, hinting at both algorithms being identically affected by the erroneous lens-modelling distortion effect.

<div align="center">RESULTS AND DISCUSSION</div>

Estimating Ice Volume from DEM Difference

Having analysed the error bar on the DEM difference, and considering that the DEMs are matched using GCPs identified on the reference orthophotograph, now consider the DEM difference for extracting snow depth and icing volume.

Icings are a seasonal phenomenon, most of the time localised along rivers, where ground topography constraints (generally sharp river channels) are the most important. The latter issue is thus most easily identified since icings form in well-defined channels carved by running water in summer and, once filled with snow, create icings through snow transformation by the liquid water seeping from the glacier from autumn to spring through the winter. This stratified ice, formed from the freezing of successive outflows (Bukowska-Jania and Szafraniec, 2005), appears at typical channel heights from 1 to 5 m, which might not be fully filled by ice but hint at thicknesses well above the measurement uncertainty from the DEM difference. Indeed, the channels concentrating icing formations are readily visible, as shown in Fig. 7.

A core assumption when computing icing and snowpack volume is that the underlying moraine topography does not evolve between the two measurement epochs. Thus, any elevation change is attributed to snow and ice accumulation alone and not to mechanical erosion of the moraine due to major flooding induced by strong outflows generated by rain events. Such an assumption is met if the reference DEM is acquired at the end of the summer season, when liquid precipitation has ended and the moraine remains frozen until the first snowfall. This assumption is usually met if the reference model of the snow-free
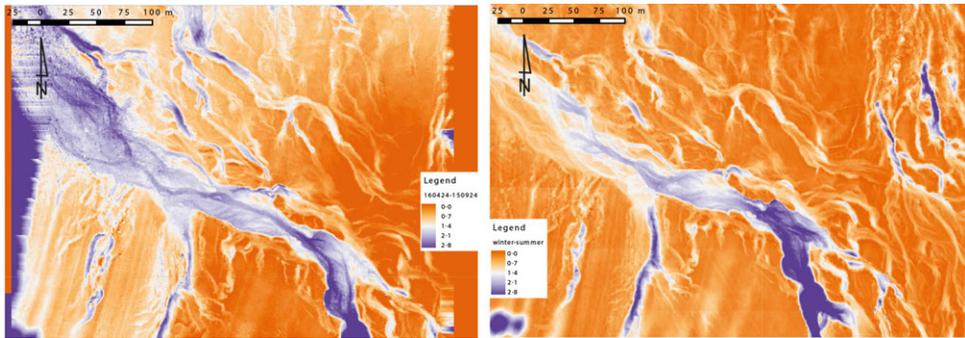
FIG. 7. Left: colour-shaded image of the DEMs generated from SfM and adjusted through a translation using GCPs. The two dates at which the data were acquired were 24th September 2015 and 24th April 2016. Right: difference of DEMs generated from lidar.

moraine topography is acquired at the end of the hydrological season – the beginning of October – although a sudden flood late in the season might require a later reference flight if the moraine topography is significantly affected. Throughout the following analysis, the hypothesis of a given moraine topography during autumn and winter is met; thus, all elevation changes are attributed to snow and ice accumulation.

Independent Estimation of Ice Volume

The volume of ice accumulated in the canyon concentrating flows from the glacier is estimated from difference of DEMs acquired at the minimum and maximum extents of the icings, integrating this difference over the canyon area. This phenomenon is indeed most visible following the main canyon concentrating the most important water fluxes.

Using zonal statistics, and computing with a GSD of $9\,\text{cm} \times 9\,\text{cm}$, $1 \cdot 1 \times 10^5 \pm 0 \cdot 2 \times 10^5\,\text{m}^3$ of water is stored in the ice margins. Past hydrological measurements yield independent estimates in close agreement with this result. Indeed, Griselin (1985) estimated a sub-glacial stream flow of $0 \cdot 005\,\text{m}^3/\text{s}$: assuming this stream flow rate to be constant throughout the winter, lasting the seven months from September to April, then the volume of water accumulating in the icings is $0 \cdot 005\,\text{m}^3/\text{s} \times 86\,400\,\text{s/day} \times 181\,\text{days} \approx 0 \cdot 78 \times 10^5\,\text{m}^3$. Considering the rough assumption of constant flow, these two figures obtained from independent sources are in surprisingly good agreement, and provide an estimate of the sub-glacial stream contribution to the hydrological budget observed at the outlet of the moraine.

Snow Distribution and Quantification

The icings accumulating in the canyon carved by the sub-glacial stream are well analysed with difference of DEMs integration since the elevation variations are well above the measurement resolution. The research then wished to assess whether the snowpack distribution over the whole moraine can be analysed similarly: the snowpack requires better elevation accuracy and is prone to misinterpretation of snow-drift accumulation if the two DEMs are not well aligned.

Unlike the glacier itself, and even less so for the slopes, the moraine, due to its complex topography, is a challenging area for snow-cover observation and monitoring.

Snow-free areas contrast with deep cornice accumulation and deep river channels filling. A few centimetres of snowfall are thus relatively small compared with, sometimes, more than 5 m of snow accumulation. However, with an accurate base DEM, areas with clearly identifiable snowdrift are the easiest topographic areas to assess snowpack height and volume. This provides the most important difference between maximum snow accumulation and snow-free ground, and makes checking possible. However, this requires that the imagery acquired provides sufficient contrast, which is not always the case given the high colour homogeneity of snow.

Snowpack dynamics is a challenging measurement at the threshold of SfM accuracy. While the changing moraine topography might be erroneously attributed to snow accumulation, most significantly the strong topographic variation requires sub-metre lateral (horizontal) positioning of one DEM with respect to the reference DEM to avoid artefacts attributed to snowdrift accumulation on the slopes of the undulations in the moraine. Such erroneous alignments are readily identified as positive accumulation on one side of the hill associated with negative height difference on the opposite slope (Fig. 6).

Climatic conditions of the 2015–2016 hydrological year considered here were, unfortunately, not well suited for such a demonstration. Indeed, although precipitation was abnormally high, most of it was liquid, making this year one of the worst in the last decade in terms of snow accumulation. The glacier snowpack was the second shallowest recorded over the last nine years. The glacier snowpack measured in April 2016 was 491 mm snow water equivalent (SWE) while the mean over the past nine years was 790 mm SWE. Consequently, little accumulation on the moraine was observed: the shallow snowpack thus provides especially poor conditions for this demonstration. Hence, this work considers, as a reference dataset, the difference of lidar DEMs (Fig. 2) acquired at the end of April 2016 (theoretically the maximum snowpack depth) and August 2016 (the reference state with the lowest snow level in the moraine). Making the overall difference between the two lidar DEMs available, accumulation areas appear clearly, specifically in the deepest canyons of the moraine. Moreover, considering the resolution and according to what was recently observed about proglacial moraine movement (Bernard et al., 2017), it is quite difficult to attribute volume differences to snow accumulation or moraine materials. Short warm-and-rainy events are known to be responsible for significant morphological changes in the proglacial moraine. Thus, it can be assumed that part of the change in volume, measured between the April and October flight campaigns, can be attributed to proglacial moraine geometric changes which occurred following the strong summer-melting outflows.

LESSONS LEARNT

This work has demonstrated the use of a COTS UAV for acquiring aerial-view photographs of a polar glacier moraine in order to observe geomorphological and snow-cover evolution between two seasons separated by six months. Due to the change of GNSS geometries inherent in the GPS and GLONASS constellations, single frequency GNSS coordinates of the camera, when each picture is taken, provide insufficient resolution for sub-metre positioning of the DEMs. Poor lateral positioning accuracy induces high DEM elevation variations due to the rough topography of the moraine, as opposed to the smooth glacier surface where lateral positioning errors only marginally impact elevation estimation. The classical approach of distributing measurement GCP targets in the field prior to flying is challenging due to the thick snow cover hiding such targets in wintertime, and the poor weather conditions, as well as soft ground, in summer preventing such GCPs remaining in the field during the long time intervals between flights. Because interest is primarily in

DEM differences, current investigations focus on exploiting natural GCPs, such as large boulders assumed not to have moved between flight sessions, for positioning successive DEMs with sub-metre relative accuracy. Systematic raster scans over a given area eases photogrammetric processing thanks to the excellent lateral overlap, but this research has not observed any limitation in photogrammetric image processing following the manual flight of the UAV when tracking elongated features such as river beds or coastlines. The technological selection of a rotating-wing UAV (multicopter) with limited battery autonomy due to the lack of aerodynamic lift is questionable. While well suited to urban and other populated areas, a fixed-wing UAV exhibits longer flight life expectancy for a given battery capacity, while the polar region offers no obstacles in terms of vegetation or manmade infrastructure. Automated flight controllers (for example, the Pixhawk, outlined in Meier et al., 2011) are readily available both for rotating- and fixed-wing UAVs, so that the latter appear better suited for the work under investigation.

Despite the work undertaken by several researchers with the goal of studying snow cover, the physical properties of snow, as well as climatic conditions in the Arctic, make measurements and even basic observations difficult to carry out. This is true whether an aerial survey or classical field observations are undertaken. Under thick snow-cover conditions, the lack of tie points and GCPs due to markers being covered by a homogeneous snow layer makes photogrammetric processing of mostly white pictures challenging when neither shadows nor rocks are visible. Moreover, if it is possible to estimate snow thicknesses, field measurements are needed to obtain additional data such as SWE by measuring snow density. It can be observed that accurate snow-cover monitoring needs a thorough simultaneous application of both photogrammetry and classical snow measurements.

CONCLUSIONS

This work assesses the use of combined UAV and SfM methods for volume quantification in an Arctic environment. More specifically, this method is well adapted to analyse short events inducing significant topographical changes – sudden rain-on-snow events washing away the snow cover or heavy snowfall – as well as quantifying icing accumulation throughout the hydrological year. Orthophotographs are well suited for quantifying snow and ice distribution in the moraine, as well as following detailed hydrological processes such as stream braiding or flow shift. However, quantifying height differences between the theoretical maximum snow accumulation and, at the opposite extreme, the end of the hydrological year when only few firm packs and icings remain, requires improvement in the positioning of DEMs. This is best addressed by better GCP use in the SfM workflow. The lidar workflow integrates GCPs as reflective target corner reflectors for matching point-cloud positions, improving the accuracy of the DEM positioning enough for snow-cover volume estimates to become relevant. The issue of snow-density measurement for converting snow-cover thicknesses to water equivalent quantities needed in a hydrological budget remains the same for all remote sensing techniques.

Snow-cover thickness and icing water equivalent can thus be measured in remote areas, but the most challenging part remains the processing of a huge quantity of data and obtaining an accurate result over a large monitored surface (in this case the whole moraine surface). The basic assumption, when measuring after the last rainfall at the end of autumn as winter sets in (end of the hydrological year, set at 1st October) for assessing icing and snow-cover volume, is that the underlying moraine topography no longer changes, and that all topographic modifications observed from lidar or SfM are due to snow and ice

accumulation. In contrast, during the melt season both ice melt and snowmelt, as well as morphological changes, are measured using DEM differences. Only by considering snow-free or snow-covered areas, as observed on the orthophotographs, can the nature of the elevation change be attributed to melting or morainic material displacement.

The flexibility of a small COTS UAV and SfM are well suited to the specific study of short-term cryosphere processes. They can be highlighted at a high spatial resolution which could be compared to lidar measurements. Moreover, rapid changes induced by climate change can be recorded thanks to the possibility of easy monitoring repeatability provided by a small COTS UAV.

Acknowledgements

References

Arnold, N. S., Rees, W. G., Devereux, B. J. and Amable, G. S., 2006. Evaluating the potential of high-resolution airborne LiDAR data in glaciology. *International Journal of Remote Sensing*, 27(6): 1233–1251.

Bangen, S. G., Wheaton, J. M., Bouwes, N., Bouwes, B. and Jordan, C., 2014. A methodological intercomparison of topographic survey techniques for characterizing wadeable streams and rivers. *Geomorphology*, 206: 343–361.

Bavay, M., Grünewald, T. and Lehning, M., 2013. Response of snow cover and runoff to climate change in high Alpine catchments of Eastern Switzerland. *Advances in Water Resources*, 55: 4–16.

Bernard, É., Friedt, J. M., Tolle, F., Griselin, M., Martin, G., Laffly, D. and Marlin, C., 2013. Monitoring seasonal snow dynamics using ground based high resolution photography (Austre Lovénbreen, Svalbard, 79°N). *ISPRS Journal of Photogrammetry and Remote Sensing*, 75: 92–100.

Bernard, É., Friedt, J. M., Tolle, F., Marlin, C. and Griselin, M., 2017. Using a small COTS UAV to quantify moraine dynamics induced by climate shift in Arctic environments. *International Journal of Remote Sensing*, 38(8–10): 2480–2494.

Bukowska-Jania, E. and Szafraniec, J., 2005. Distribution and morphometric characteristics of icing fields in Svalbard. *Polar Research*, 24(1–2): 41–53.

Cook, K. L., 2017. An evaluation of the effectiveness of low-cost UAVs and structure from motion for geomorphic change detection. *Geomorphology*, 278: 195–208.

Deems, J. S., Painter, T. H. and Finnegan, D. C., 2013. Lidar measurement of snow depth: a review. *Journal of Glaciology*, 59(215): 467–479.

Eckerstorfer, M. and Christiansen, H. H., 2011. The high Arctic maritime snow climate in central Svalbard. *Arctic, Antarctic, and Alpine Research*, 43(1): 11–21.

Eltner, A. and Schneider, D., 2015. Analysis of different methods for 3D reconstruction of natural surfaces from parallel-axes UAV images. *Photogrammetric Record*, 30(151): 279–299.

Gindraux, S., Boesch, R. and Farinotti, D., 2017. Accuracy assessment of digital surface models from unmanned aerial vehicles' imagery on glaciers. *Remote Sensing*, 9(2). 15 pages.

Griselin, M., 1985. Les marges glacées du Loven Est, Spitsberg: un milieu original lié aux écoulements sous-glaciaires. *Revue de Géographie Alpine*, 73(4): 389–410.

Hagen, J. O., Kohler, J., Melvold, K. and Winther, J.-G., 2003. Glaciers in Svalbard: mass balance, runoff and freshwater flux. *Polar Research*, 22(2): 145–159.

Hagen, J. O., Eiken, T., Kohler, J. and Melvold, K., 2005. Geometry changes on Svalbard glaciers: mass-balance or dynamic response? *Annals of Glaciology*, 42: 255–261.

Hock, R., 2003. Temperature index melt modelling in mountain areas. *Journal of Hydrology*, 282(1–4): 104–115.

James, M. R. and Robson, S., 2014. Mitigating systematic error in topographic models derived from UAV and ground-based image networks. *Earth Surface Processes and Landforms*, 39(10): 1413–1420.

KRŠÁK, B., BLIŠŤAN, P., PAULIKOVÁ, A., PUŠKÁROVÁ, P., KOVANIČ, Ľ., PALKOVÁ, J. and ZELIZŇAKOVÁ, V., 2016. Use of low-cost UAV photogrammetry to analyze the accuracy of a digital elevation model in a case study. *Measurement*, 91: 276–287.

LUCIEER, A., DE JONG, S. and TURNER, D., 2014a. Mapping landslide displacements using structure from motion (SfM) and image correlation of multi-temporal UAV photography. *Progress in Physical Geography*, 38(1): 97–116.

LUCIEER, A., TURNER, D., KING, D. H. and ROBINSON, S. A., 2014b. Using an unmanned aerial vehicle (UAV) to capture micro-topography of Antarctic moss beds. *International Journal of Applied Earth Observation and Geoinformation*, 27(A): 53–62.

MEIER, L., TANSKANEN, P., FRAUNDORFER, F. and POLLEFEYS, M., 2011. Pixhawk: a system for autonomous flight using onboard computer vision. *IEEE International Conference on Robotics and Automation (ICRA)*: 2992–2997.

MICMACIGN, 2017. https://github.com/micmacIGN [Accessed: 22nd September 2017].

NIEDERHEISER, R., MOKROŠ, M., LANGE, J., PETSCHKO, H., PRASICEK, G. and OUDE ELBERINK, S. J., 2016. Deriving 3D point clouds from terrestrial photographs – comparison of different sensors and software. *International Archives of the Photogrammetry, Remote Sensing and Spatial Information Sciences*, 41(B5): 685–692.

NOLAN, M., LARSEN, C. and STURM, M., 2015. Mapping snow depth from manned aircraft on landscape scales at centimeter resolution using structure-from-motion photogrammetry. *The Cryosphere*, 9(4): 1445–1463.

NORWEGIAN POLAR INSTITUTE, 2010. *Toposvalbard*. http://toposvalbard.npolar.no/ See also: http://geodata.npolar.no/arcgis/rest/services/Basisdata/NP_Ortofoto_Svalbard_WMTS_25833/MapServer/WMTS? [Accessed: 22nd September 2017].

NOWAK, A. and HODSON, A., 2013. Hydrological response of a high-Arctic catchment to changing climate over the past 35 years: a case study of Bayelva watershed, Svalbard. *Polar Research*, 32(1). 16 pages.

OERLEMANS, J., 2005. Extracting a climate signal from 169 glacier records. *Science*, 308(5722): 675–677.

PANHOLZER, H. and PROKOP, A., 2013. Wedge-filtering of geomorphologic terrestrial laser scan data. *Sensors*, 13(2): 2579–2594.

PIERROT-DESEILLIGNY, M., 2017. *Micmac, Apero, Pastis and Other Beverages in a Nutshell*! https://github.com/micmacIGN/Documentation/blob/master/DocMicMac.pdf. 457 pages (in French and English). [Accessed: 21st September 2017].

PROKOP, A., 2008. Assessing the applicability of terrestrial laser scanning for spatial snow depth measurements. *Cold Regions Science and Technology*, 54(3): 155–163.

PROKOP, A. and PANHOLZER, H., 2009. Assessing the capability of terrestrial laser scanning for monitoring slow moving landslides. *Natural Hazards and Earth System Science*, 9(6): 1921–1928.

PROKOP, A., SCHIRMER, M., RUB, M., LEHNING, M. and STOCKER, M., 2008. A comparison of measurement methods: terrestrial laser scanning, tachymetry and snow probing for the determination of the spatial snow-depth distribution on slopes. *Annals of Glaciology*, 49: 210–216.

PROKOP, A., SCHÖN, P., SINGER, F., PULFER, G., NAAIM, M., THIBERT, E. and SORUCO, A., 2015. Merging terrestrial laser scanning technology with photogrammetric and total station data for the determination of avalanche modeling parameters. *Cold Regions Science and Technology*, 110: 223–230.

RACHLEWICZ, G., 2010. Paraglacial modifications of glacial sediments over millennial to decadal time-scales in the high Arctic (Billefjorden, central Spitsbergen, Svalbard). *Quaestiones Geographicae*, 29(3): 59–67.

RADIĆ, V., BLISS, A., BEEDLOW, A. C., HOCK, R., MILES, E. and COGLEY, J. G., 2014. Regional and global projections of twenty-first century glacier mass changes in response to climate scenarios from global climate models. *Climate Dynamics*, 42(1–2): 37–58.

REES, W. G. and ARNOLD, N. S., 2007. Mass balance and dynamics of a valley glacier measured by high-resolution LiDAR. *Polar Record*, 43(4): 311–319.

SCHÖBER, J., SCHNEIDER, K., HELFRICHT, K., SCHATTAN, P., ACHLEITNER, S., SCHÖBERL, F. and KIRNBAUER, R., 2014. Snow cover characteristics in a glacierized catchment in the Tyrolean Alps – improved spatially distributed modelling by usage of Lidar data. *Journal of Hydrology*, 519(D): 3492–3510.

SOBOTA, I., 2016. Icings and their role as an important element of the cryosphere in high Arctic glacier forefields. *Bulletin of Geography (Physical Geography series)*, 10(1): 81–93.

WACKROW, R. and CHANDLER, J. H., 2008. A convergent image configuration for DEM extraction that minimises the systematic effects caused by an inaccurate lens model. *Photogrammetric Record*, 23(121): 6–18.

WACKROW, R. and CHANDLER, J. H., 2011. Minimising systematic error surfaces in digital elevation models using oblique convergent imagery. *Photogrammetric Record*, 26(133): 16–31.

WESTOBY, M. J., BRASINGTON, J., GLASSER, N. F., HAMBREY, M. J. and REYNOLDS, J. M., 2012. 'Structure-from-motion' photogrammetry: a low-cost, effective tool for geoscience applications. *Geomorphology*, 179: 300–314.

WHITEHEAD, K., MOORMAN, B. and WAINSTEIN, P., 2014. Measuring daily surface elevation and velocity variations across a polythermal Arctic glacier using ground-based photogrammetry. *Journal of Glaciology*, 60(224): 1208–1220.

WIESMANN, S., STEINER, L., POZZI, M., BOZZINI, C., BAUDER, A. and HURNI, L., 2012. Reconstructing historic glacier states based on terrestrial oblique photographs. *AutoCarto 2012*, Columbus, Ohio, USA. 14 pages.

WRIGHT, A. P., 2005. *The Impact of Meltwater Refreezing on the Mass Balance of a High Arctic Glacier*. Doctoral thesis, University of Bristol, Bristol, UK. 265 pages.

Résumé

Ce travail s'intéresse aux méthodes permettant d'établir la contribution de la moraine pro-glaciale dans les écoulements d'un petit hydrosystème arctique. Des MNTs à haute résolution spatiale, et à différentes saisons, sont nécessaires pour estimer le volume de glace et de neige accumulés dans la moraine qui participent ensuite aux écoulements en période de fonte. Le LIDAR est actuellement la méthode de référence pour générer des MNTs: cet instrument hautement spécialisé fourni la meilleure résolution. Nous considérons ici, en complément, l'utilisation d'un drone (de type DJi Phantom3) pour l'acquisition d'images aériennes, combiné avec des méthodes de traitement des images par photogrammétrie (Structure from Motion). La différence de MNTs entre des jeux de données acquis en avril (maximum d'accumulation neigeux) et en septembre (absence de neige ou manteau neigeux minimal) permet de quantifier des volumes, attribués à la fois au manteau neigeux et aux phénomènes d'«icings». Des acquisitions répétées sur un pas de temps court permettent par ailleurs de mettre en évidences les processus liés au stockage de la neige dans la moraine et à la fonte du manteau neigeux.

Zusammenfassung

Es werden Methoden zur Abschätzung des Beitrags einer eiszeitlichen Moräne zum Wasserhaushalt eines arktischen Gletschers untersucht. Hierzu werden hochauflösende Höhenmodelle für verschiedene Jahreszeiten benötigt, um das Volumen von Eis und Schnee zu ermitteln, das sich im Winter in diesem Teil des Wassereinzugsgebiets bildet und während der Schneeschmelze in Flüsse abfließt. Mit Lidar werden aktuell die höchsten Auflösungen für die Generierung Digitaler Höhemmodelle (DHM) erzielt. Dieser Beitrag beschreibt eine ergänzende Erfassung mit einer kommerziellen DJI Phantom 3 Drohen (UAV) für die Erfassung von Luftbildern und die nachfolgende Auswertung mit Structure-From-Motion (SfM) für die DHM Berechnung. Die Differenzen zwischen Höhenmodellen aus April (maximale Anreicherung mit Schnee) und September (minimale Schneebedeckung) ergeben eine Volumendifferenz entweder aus Schneebedeckung oder Eisbildung. Wiederholte Messungen über eine kurze Periode zeigen die Prozesse der Schneespeicherung in der Moräne und die Dynamik des Schmelzvorganges auf.

Resumen

Se estudian métodos para evaluar la contribución de la morrena pro glacial al balance hídrico de un glaciar ártico. Para estimar el volumen de hielo y nieve acumulados durante el invierno en esta parte de la cuenca hidrográfica y liberarlos en los ríos durante la temporada de fusión se necesitan modelos de elevación de alta resolución espacial en diferentes estaciones. El Lidar ofrece actualmente la más alta resolución para la generación de modelos digitales de elevación (MED). En este trabajo se estudia el uso complementario de un vehículo aéreo no tripulado (UAV) del tipo DJI Phantom 3 para la adquisición de fotografía aérea, combinado con métodos fotogramétricos para el cálculo del MED. Las diferencias de MED entre los conjuntos de datos adquiridos en abril (acumulación máxima de nieve) y septiembre (cobertura mínima de nieve) producen una

diferencia de volumen atribuida a la cubierta de nieve o a la formación de hielo. Mediciones repetidas durante un corto período destacan los procesos de almacenamiento de la cubierta de nieve en la morrena y la dinámica de fusión.

摘要

本文探讨了冰川外缘的冰碛对北极冰川水总量贡献的评估方法。应用不同季节的高空间分辨率数字高程模型, 可以估计所研究区域中冬季累积的冰雪, 以及在融化季节中排入河流的量。激光扫描技术是目前可以提供最高分辨率数字高程模型 (DEM) 的方法。本文考虑了另一种方法, 即使用市场上可购买的 DJI Phantom 3 专业无人机 (UAV) 进行航空摄影, 结合运动恢复结构 (SfM) 进行 DEM 计算与获取。4月份 (最大积雪)获得的数据与9月份(最低积雪)之间的 DEM 的差异, 即为雪覆盖或冰雪形成所造成的体积差异。在短时间范围内进行重复的测量, 可展现出冰碛和融化的动态过程中之雪储存量。